# Supporting Information Appendix

***Potential for Western United States Seasonal Snowpack Prediction***

***Authors:*** *Sarah B. Kapnick, Xiaosong Yang, Gabriel A. Vecchi, Thomas L. Delworth, Rich Gudgel, Sergey Malyshev, P.C.D. Milly, Elena Shevliakova, Seth Underwood, Steven A. Margulis*

## Gridding Process for Observations and Model Output

After quality control, snowpack point observations were gridded to the 200, 50, and 25 km AOGCM grids using a nearest neighbor approach where stations in each grid cell were grouped and averaged to form gridded values (1). At coarser scales, this appears to grossly overestimate SWE (Fig. 1) because values for zero snow (where stations do not exist) are not included. The simulated AOGCM SWE was similarly regridded from one model resolution to another using a linear interpolation for comparison with observations on a common grid (Figs. 3, 4). Regional comparisons are made only in gridcells with positive SWE climatologies from the AOGCMs (Fig. S1), removing those points in Fig. 1 where the station regridding process produces snow almost everywhere. We assume that the regridding process captures regional interannual variability in snowpack for prediction skill validation found in Fig. 3. This highlights the need for either high resolution (for regridding to coarser grids) or scale-independent observational data products for model evaluation.

## Normalized Regional Snowpack Anomaly

Due to differences in resolution affecting elevation height (Fig. S1) and potentially limiting SWE magnitudes (Figs. 1,S1,S2), we use a measure of SWE anomalies (time series example shown in

Fig. S8) normalized by each region's mean SWE for across-model comparisons and prediction skill:

$$\text{normalized anomaly} = \frac{x(t)-\bar{x}}{\bar{x}} \qquad \text{(Equation S1)}$$

Where $x(t)$ represents the SWE at time $t$ and $\bar{x}$ represents the mean SWE.

**Climate Indices**

Various climate indices have been used previously to explore intraseasonal covariance with WUS snowpack variability (2-8). Here we use the monthly observed values of the Pacific / North American (PNA) pattern, Multivariate El Niño Southern Oscillation (ENSO) index, and Pacific Decadal Oscillation (PDO) index. The June PNA was downloaded from the NOAA Climate Prediction Center (information described here: http://www.cpc.ncep.noaa.gov/data/teledoc/telecontents.shtml). The PNA index is a measure of the state of the atmosphere, based on atmospheric 500 mb height anomalies standardized by the 1981-2010 climatology. We use the Multivariate ENSO index based on 6 variables across the Pacific region reflecting the atmosphere and ocean states: sea-level pressure, zonal and meridional components of the surface wind, sea surface temperature, surface air temperature, and total cloudiness fraction. The May/June ENSO value was downloaded from the NOAA Earth System Research Laboratory (https://www.esrl.noaa.gov/psd/enso/mei/). ENSO values are standardized by the 1950-1993 climatology. The PDO index was downloaded from the University of Washington (http://research.jisao.washington.edu/pdo/) (12). Data was accessed for all indices on May 23, 2016 and again for the PDO on February 7, 2017.

The standardized observed climate indices available on July 1 are used to determine if the climate state on July 1 has information for prediction of spring snowpack 8 months later. The

covariance of winter climate indices with April 1 snowpack (2-7) suggests that there may be prediction skill, but has not previously been quantified. We use this straightforward static statistical prediction in comparison with our dynamics AOGCM prediction to determine if the dynamical system provides additional information beyond the initial climate state to improve prediction skill.

**Gridded Non-Snow Observations**

Temperature and total precipitation observations were obtained from the University of East Anglia Climate Research Unit (CRU) for comparison with model output. Version ts3.2.3 (https://crudata.uea.ac.uk/cru/data/hrg/) is used in our analysis of November-February temperature and precipitation, spanning November 1980 through February 2015. (Data for 2016 is presently unavailable). For calculating storm track prediction skill, the v-component of winds was obtained at 850 mb from ERA-Interim, a reanalysis product produced by the European Centre for Medium-Range Weather Forecasts (10) for November 1980 through February 2015 for consistency.

**Storm Track Definition**

In the midlatitudes, concentrated regions of storminess are regularly found during the winter. These regions are referred to as storm-tracks (13). They have high concentrations of disturbing meridional winds (northward or southward) throughout the atmospheric column. Here we choose to define storm tracks by 6-hourly values of the v-component of 850 mb winds because we are interested in the influence of storms over the land surface in the mountains. We use a storm track index previously documented (9), where:

$$\text{storm track index} = \sqrt{\frac{1}{N}\sum_{t=1}^{N}[x(t+24\text{hr}) - x(t)]^2} \qquad \text{(Equation S2)}$$

where N is the sample size in days of each season (120 or 121 in a leap year), x is the climate variable defining storms (here we use the v-component of 850 mb winds), $t$ is time, and $t + 24\text{hr}$ represents a time step 24 hours later than $t$. We focus our storm track seasonal prediction on the months important for March snowpack development: November through February. Storm track predictive skill is therefore provided 4 months in advance (since it is initialized July 1).

**Ensemble Spread Characterization**

Results based on ensemble means alone obscure valuable information about a prediction system and the range of possible outcomes in an ensemble system. A coherence index like that defined in (11,14) can provide us with an assessment of the spread in individual ensemble members and how the ensemble spread relates to the spread in interannual variability in the ensemble mean. Similarly to (11,14), we define a coherence index $\Omega(\text{snow})$ for each model as:

$$\Omega(\text{snow}) = \frac{E*\sigma^2_{\text{interann}} - \sigma^2_{\text{full}}}{(E-1)\sigma^2_{\text{full}}} \qquad \text{(Equation S3)}$$

$\sigma^2_{\text{full}}$ is the variance across all individual prediction values ($SWE_j$) for all E ensemble members ($E = 10$ for the 200 km and $E = 12$ for the 50 and 25 km models) and all 36 years, giving $E * 36$ data points:

$$\sigma^2_{\text{full}} = \frac{1}{E*36-1}\sum_{j=1}^{E*36}\left|SWE_j - \bar{\mu}\right|^2 \qquad \text{(Equation S4)}$$

$\bar{\mu}$ is the mean SWE for all ensembles and all years (represented in Fig. 1).

$\sigma^2_{\text{interann}}$ is the variance of ensemble annual mean values across all 36 years (the interannual variability of the ensemble mean prediction for 1981-2016):

$$\sigma^2_{\text{interann}} = \frac{1}{35}\sum_{i=1}^{36}|\mu_i - \bar{\mu}|^2 \qquad \text{(Equation S5)}$$

where $\mu_i$ is the ensemble mean SWE for a given year i.

If all of the E ensemble members produce the same result, the two variance calculations are the same and $\Omega(\text{snow}) = 1$. If the individual ensemble members for each year are independent, then $\sigma^2_{\text{interann}}$ reduces to $\sigma^2_{\text{full}}/\text{E}$ and $\Omega(\text{snow}) = 0$. This metric is useful to understand spatial differences in prediction coherence. Higher values imply more coherence—either due to lower modeled internal variability (potentially reflecting the true real-world natural variability) or a prediction system tendency to a solution.

**Test of How A Model Predicts Itself Versus Observations**

Prediction system bias may increase the likelihood of a specific solution (also known as a systematic bias). We quantify this tendency, by calculating how well the models predict themselves. Instead of calculating how the ensemble mean predicts observations, we isolate each individual ensemble member to see how the remaining multi-ensemble mean predicts it (using a Spearman correlation across all 36 years). These 10 (200 km model) or 12 (50, 25 km models) solutions are averaged to produce a measure of the model's ability to predict itself. Higher correlation values for the model predicting itself relative to its ability to predict observations suggests a systematic prediction system bias leading to a tendency towards a solution. This does

not identify what causes this bias however. This test gives hope that future prediction system compositions can be developed to improve the ability of the model to predict observations.

**References**


1. Pavelsky TM, Kapnick S, Hall A (2011) Accumulation and melt dynamics of snowpack from a multiresolution regional climate model in the central Sierra Nevada, California. *J Geophys Res Atmos* 116(D16), doi:10.1029/2010JD015479.
2. McCabe GJ, Dettinger D (2002) Primary modes and predictability of year-to-year snowpack variations in the western United States from teleconnections with Pacific Ocean climate. *J Hydrometeo* 3(1):13-25.
3. Seager R, Kushnir Y, Nakamura J, Ting M, Naik N (2010) Northern Hemisphere winter snow anomalies: ENSO, NAO and the winter of 2009/10. *Geophys Res Lett* 37(14):L14703.
4. Clark MP, Serreze MC, McCabe GJ (2001) Historical effects of El Nino and La Nina events on the seasonal evolution of the montane snowpack in the Columbia and Colorado River Basins. *Water Resour Res* 37(3):741-757.
5. Cayan DR (1996) Interannual climate variability and snowpack in the western United States. *J Climate* 9(5):928-948.
6. Mote PW (2006) Climate-driven variability and trends in Mountain Snowpack in Western North America. *J Climate* 19(23):6209-6220.
7. Abatzoglou JT (2011) Influence of the PNA on declining mountain snowpack in the Western United States. *Int J Climatol* 31(8):1135-1142.
8. Guan B, Waliser DE, Molotch NP, Fetzer EJ, Neiman PJ (2012) Does the Madden–Julian oscillation influence wintertime atmospheric rivers and snowpack in the Sierra Nevada? *Mon Weath Rev* 140(2):325-342.
9. Yang X, et al. (2015) Seasonal predictability of extratropical storm tracks in GFDL's high-resolution climate prediction model. *J Climate* 28(9):3592
10. Dee DP, et al. (2011) The ERA‐Interim reanalysis: Configuration and performance of the data assimilation system. *Quart J Roy Meteor Soc* 137(656):553-597.
11. Koster RD, Suarez MJ, Heiser M (2000) Variance and predictability of precipitation at seasonal-to-interannual timescales. *J Hydrometeo* 1(1):26-46.
12. Mantua NJ, Hare SR, Zhang Y, Wallace JM, Francis RC (1997) A Pacific interdecadal climate oscillation with impacts on salmon production. *Bull Amer Meteo Soc* 78(6):1069-1079.
13. Hoskins, BJ, Valdes, PJ (1990) On the existence of storm-tracks. *J Atmos Sci*, *47*(15):1854-1864.
14. Koster RD, et al. (2006) GLACE: the global land–atmosphere coupling experiment. Part I: overview. *J Hydrometeo* 7(4):590-610.

## Supporting Figures

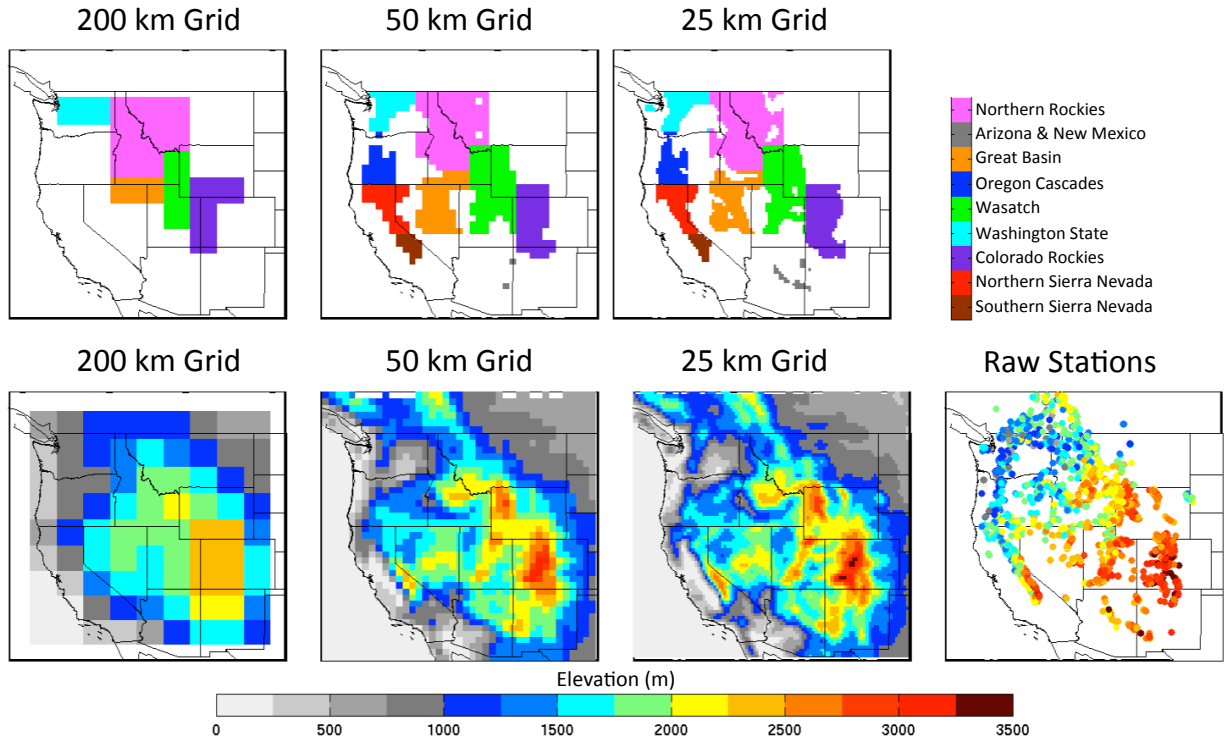


**Fig. S1.** Mountain regions for regional analysis (top) and elevations across model simulations and station observations (bottom). Note that for the 200 km model, narrow mountain ranges (Sierra Nevada, Oregon Cascades, Arizona and New Mexico) are not resolved.

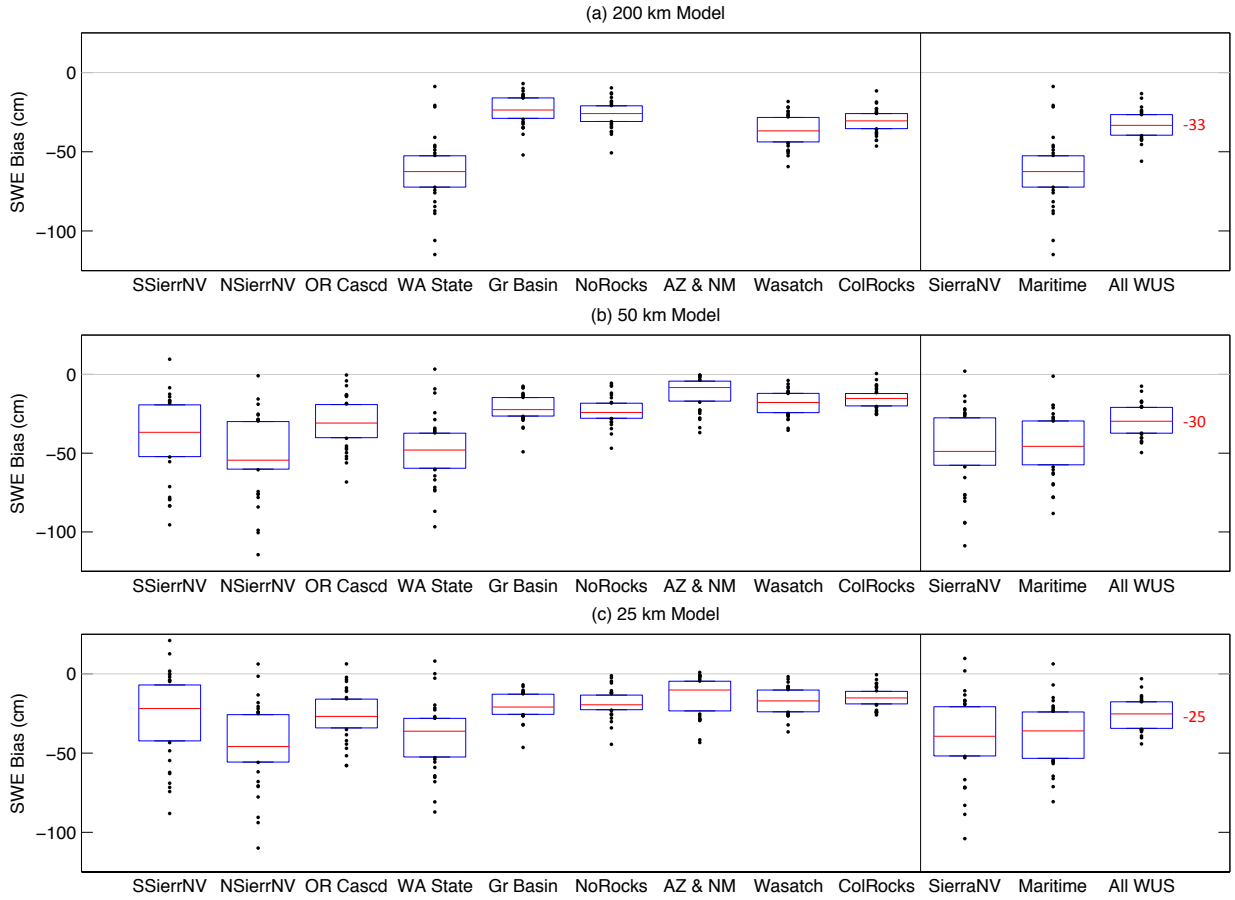


**Fig. S2. Bias in Simulated Snowpack.** Box and whisker plot of bias in regional March snow water equivalent (SWE) for 1981-2016. Regional SWE calculated for each region shown in Fig. S1. Bias calculated as simulated regional SWE minus observed regional SWE. Red line shows the median, top and bottoms of the filled boxes for the 25$^{th}$ and 75$^{th}$ percentiles. Outliers plotted by black dots.

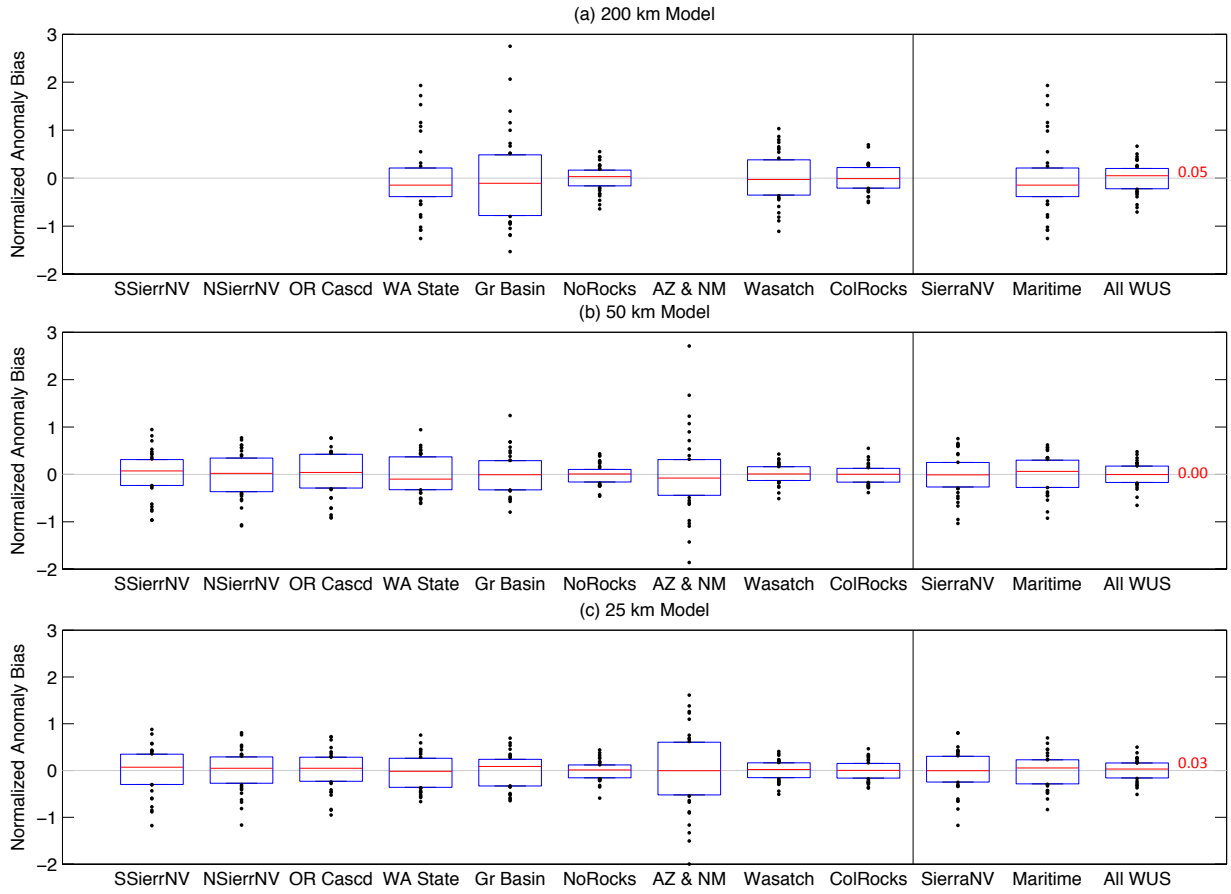


**Fig. S3: Bias in Simulated Normalized Snowpack Anomalies.** Same as Fig. S2, but for normalized snowpack anomalies (Equation S1).

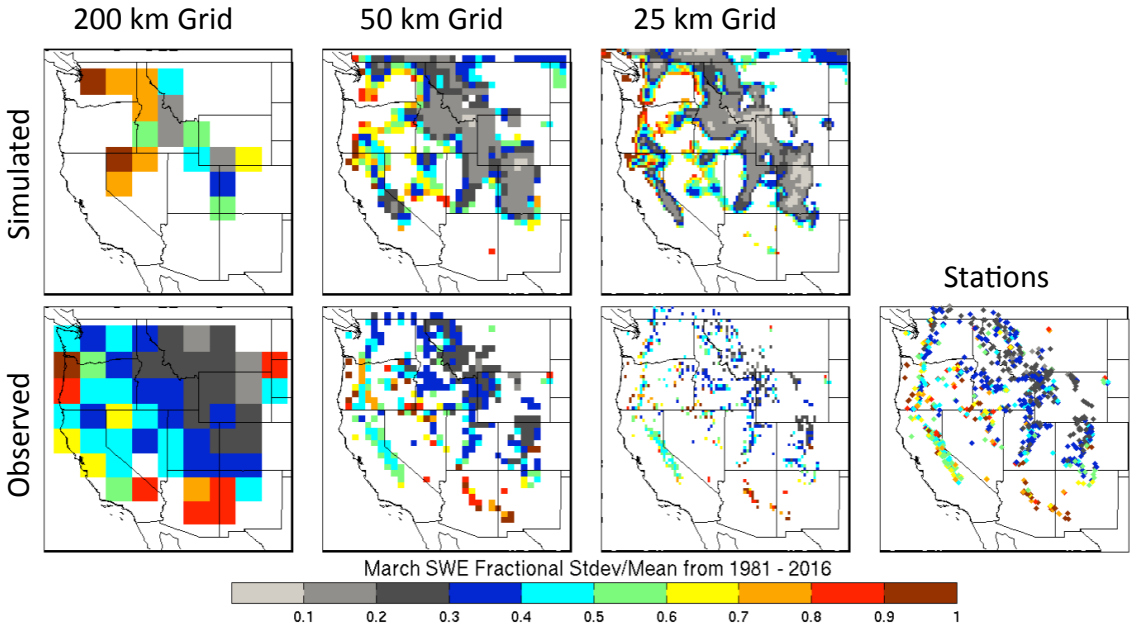


**Fig. S4.** Interannual variability of March snow water equivalent (SWE) normalized by climatology (fraction of standard deviation of ensemble mean SWE divided by mean SWE climatology) for 1981-2016. As in Fig. 2, points have been masked for only those with a minimum of 1 cm of SWE in the climatology.

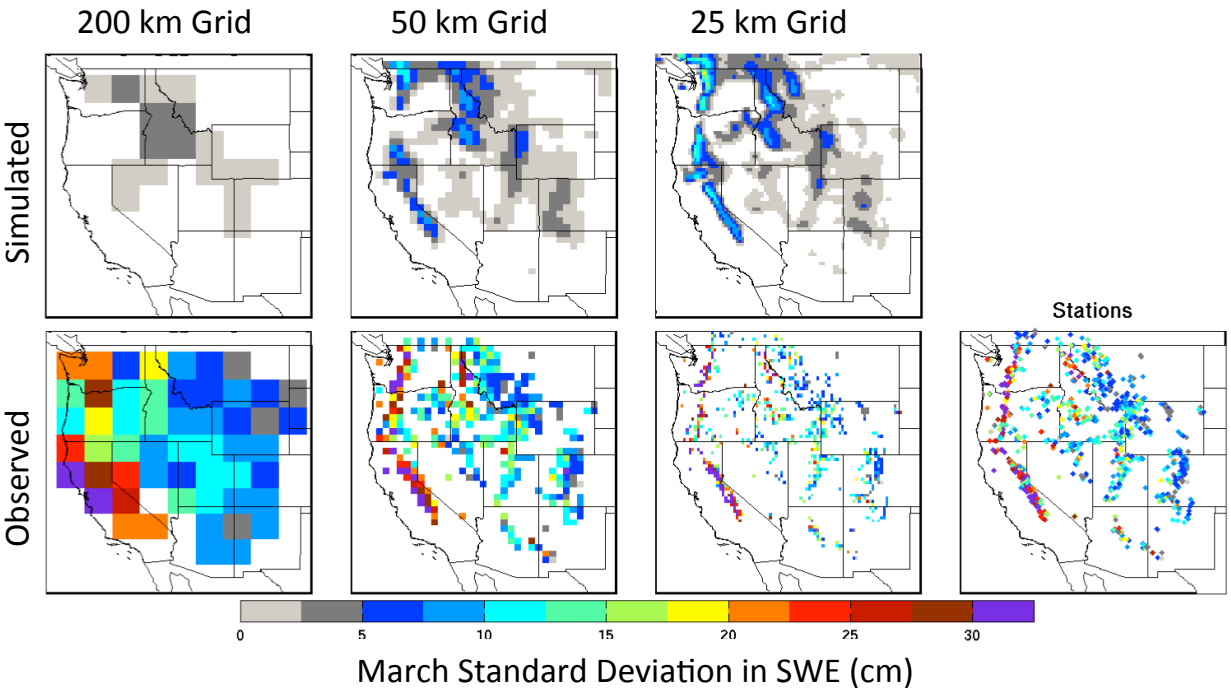


**Fig. S5.** Interannual variability of the ensemble mean snow water equivalent (SWE) for the month of March 1981-2016. As in Figure S4, but without normalization.

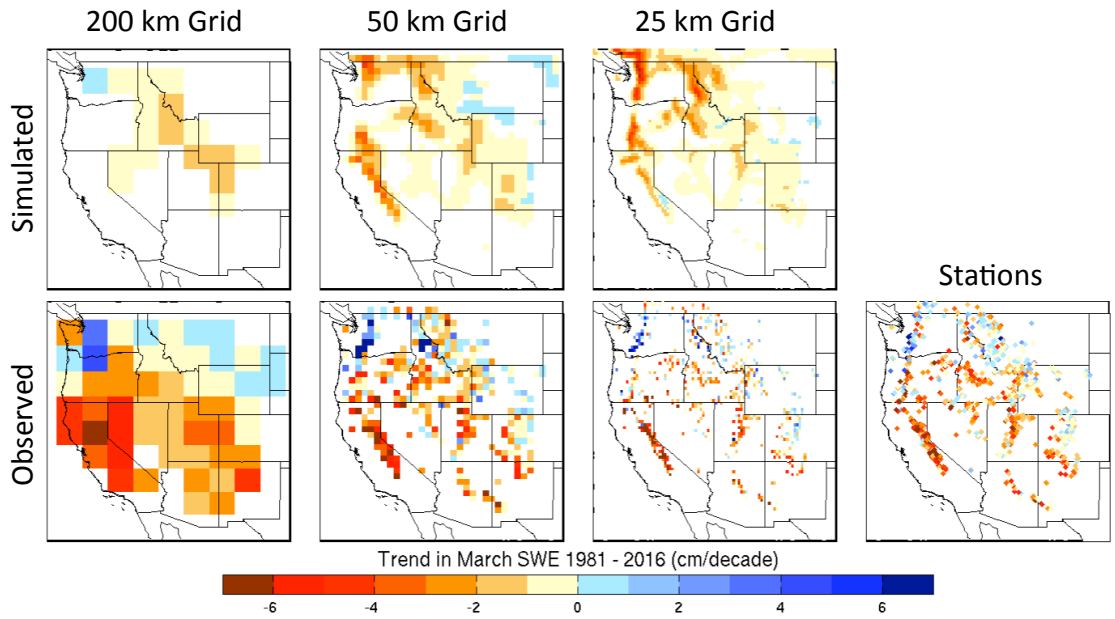


**Fig. S6.** Trend in March snow water equivalent (SWE) from 1981-2016 in observations and native model grids. As in Fig. 2, points have been masked for only those with a minimum of 1 cm of SWE in the climatology.

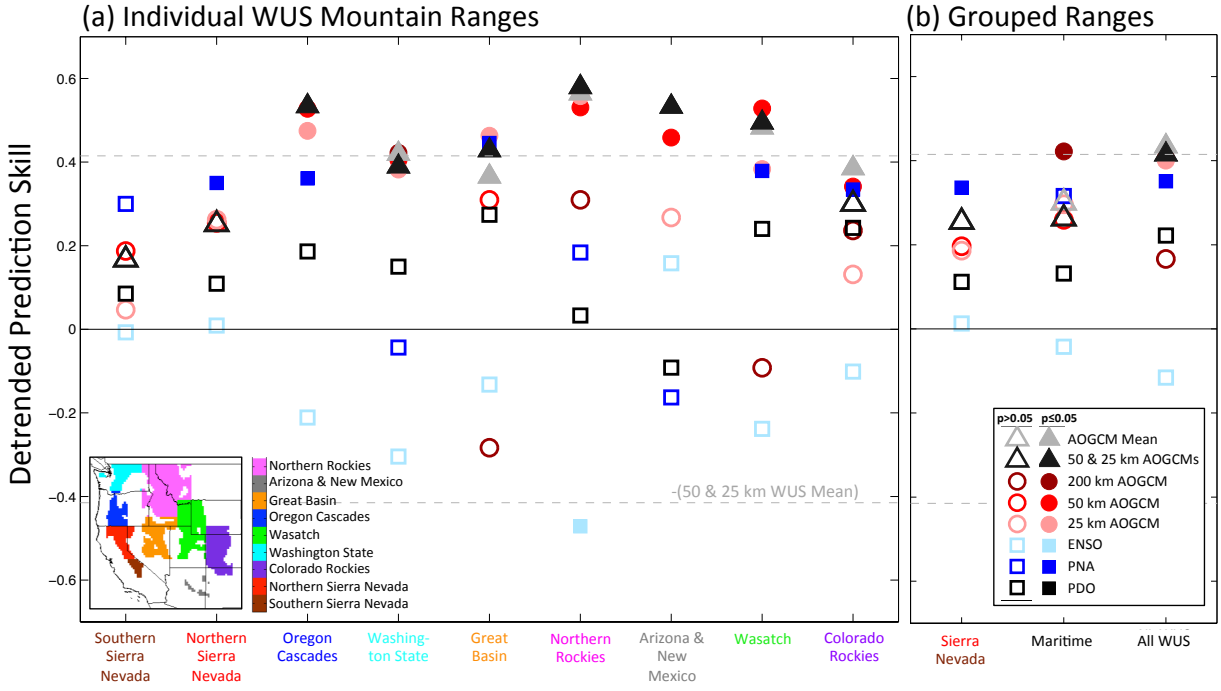


**Fig. S7.** Detrended regional predictive skill of models and climate indices. As in Fig. 3 but for variables with the linear trend removed.

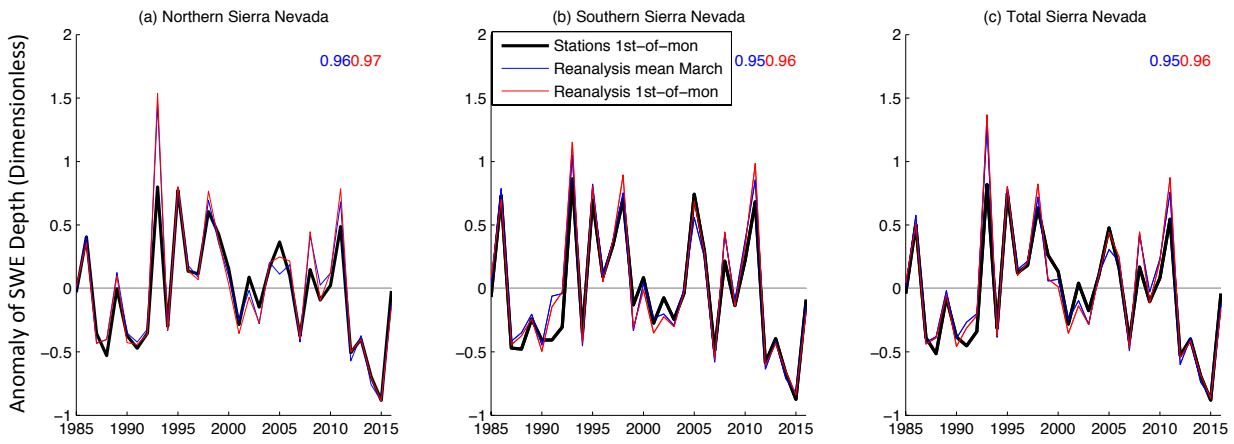


**Fig. S8: Comparison of Northern and Southern Sierra Snowpack Estimates.** Northern (a), Southern (b), and Total (c) Sierra Nevada snowpack anomalies from 1985-2016 estimated from snow stations (Figure S1) and snow reanalysis. Anomalies calculated as the deviation in snow water equivalent (SWE) from the mean divided by the mean value (Eq. 1). Correlations provided in the upper right hand corners for the station product versus the two reanalysis estimates: mean March SWE (blue) and the averaged 1st of March and 1st of April SWE values (red).

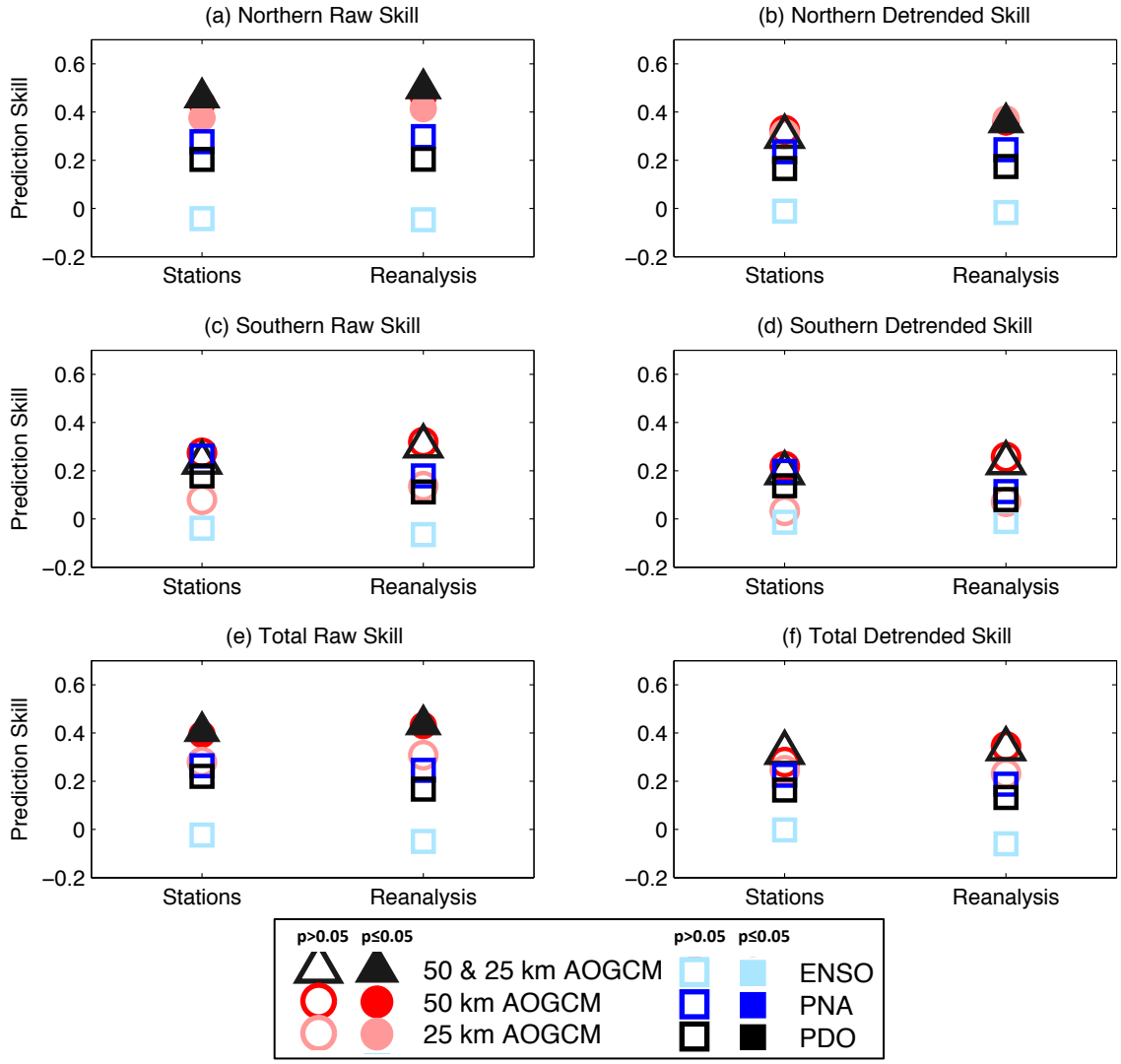


**Fig. S9: Comparison of Seasonal Prediction Skill from Two Estimates of Sierra Snowpack.** Estimates provided for AOGCM prediction system skill from 1985-2016 for Northern (a,b), Southern (c,d), and Total (e,f) Sierra Nevada snowpack. (a,c,e) provide prediction skill of "raw" anomalies of snowpack. (b,d,f) provide prediction skill for detrended anomalies. Mean March snowpack reanalysis values used for "reanalysis". Note: the station prediction skill in this figure differs in its start date (1985) from Figs. 3,S7 (1981).

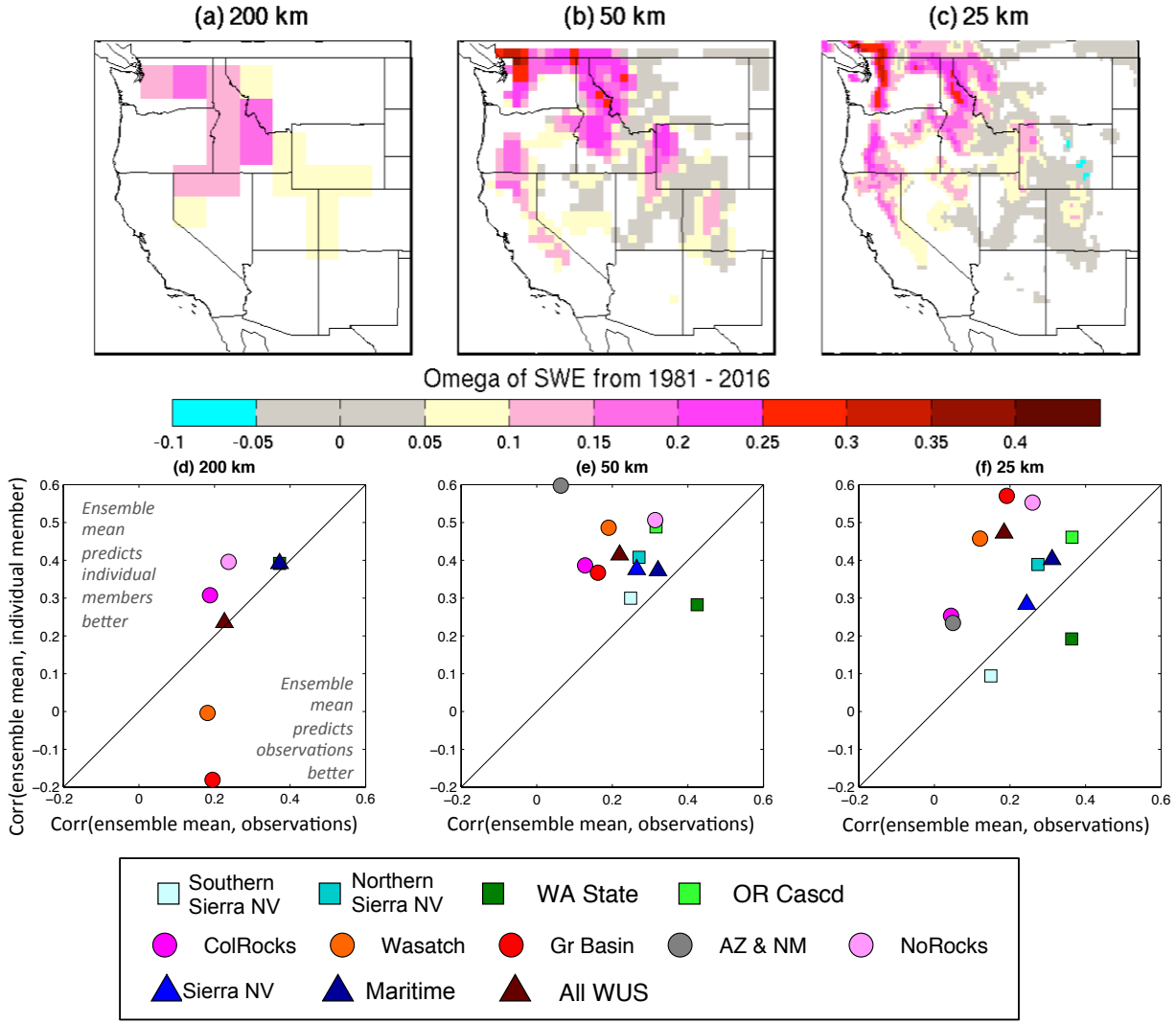


**Fig. S10.** Omega coherence index for each model (*a-c*). Larger values of omega reflect greater coherence in ensemble member outcomes whereas values approaching zero reflect greater independence in ensemble members. Masked for snow water equivalent (SWE) less than 1 cm as in Fig. 2. Perfect model calculations (*d-f*) to compare the correlation between ensemble mean versus observations (x-axis) and ensemble mean versus individual ensemble member (y-axis). See Methods for explanation of calculations.

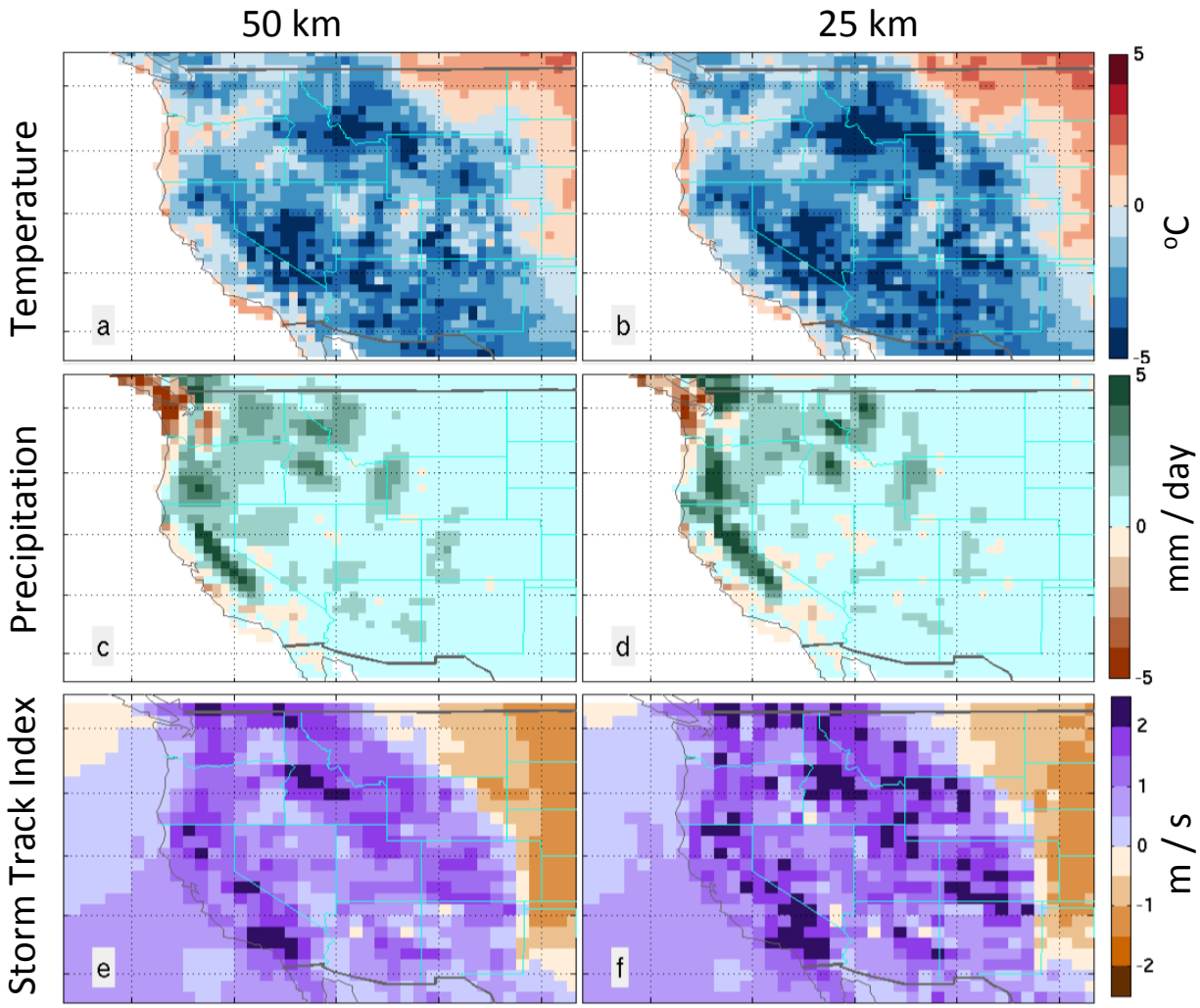


**Fig. S11.** 50 km model (left) and 25 km model (right) bias (AOGCM – observed) in November 1980 – February 2016 seasonal (November through February): temperature (*a,b*), precipitation (*c,d*) and storm track index (*e,f*) measured by standard deviation of the standard deviation of filtered daily v850.